

# Aluminum Hydride as a Fuel Supplement to Nanothermites

G. Young\*

*U.S. Naval Surface Warfare Center, Indian Head, Maryland 20640*

and

K. Sullivan,<sup>†</sup> N. Piekielek,<sup>‡</sup> and M. R. Zachariah<sup>§</sup>

*University of Maryland, College Park, Maryland 20740*

DOI: 10.2514/1.B34988

An experimental study was conducted in which aluminum hydride (alane,  $\text{AlH}_3$ ) replaced nanoaluminum incrementally as a fuel in a nanocomposite thermite based on  $\text{CuO}$ ,  $\text{Bi}_2\text{O}_3$ , and  $\text{Fe}_2\text{O}_3$ . Pressure cell and burn tube experiments demonstrated enhancements in absolute pressure, pressurization rate, and burning velocity when micron-scale aluminum hydride was used as a minor fuel component in a nanoaluminum–copper-oxide thermite mixture. Peak pressurization rates were found when the aluminum hydride made up about 25% of the fuel by mole. Pressurization rates increase by a factor of about two with the addition of  $\text{AlH}_3$ , whereas burn tube velocities increase by about 25%. The enhancement in pressurization rate appears to be primarily a result of the increased pressure associated with the  $\text{AlH}_3$  decomposition in the nanocomposite thermite system and an enhancement in convective heat transfer. Similar experiments were conducted with micron-scale aluminum in place of the aluminum hydride, which resulted in a reduction of all the previously mentioned parameters with respect to the baseline nanoaluminum–copper-oxide thermite. The addition of any amount of alane to iron oxide based thermite resulted in a reduction in performance in pressure cell testing. The performance of  $\text{Bi}_2\text{O}_3$  based thermite was largely unaffected by alane until alane became the majority fuel component. These results have been found to correlate with changes in the combustion mechanism through equilibrium calculations.

## I. Introduction

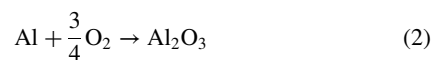
ALUMINUM hydride or alane is an interesting material for a wide variety of applications. It has been studied as a potential fuel in rocket propellants, airbreathing propulsion systems, and explosives and as a hydrogen storage medium. There are as many as six crystalline phases of alane, of which  $\alpha$ -alane is the most stable and is also the subject of this work [1,2].

Whereas alane is an interesting material for a wide variety of applications, a relatively small amount of literature exists on its combustion behavior. Sinke et al. [3] determined the heat of formation as  $-2.7$  kcal/mol by bomb calorimetry in one of the earliest publications on alane. There have been a number of studies involving the decomposition of the various polymorphs of alane under nonisothermal conditions, but these are typically conducted at very low heating rates [4–8]. In this study, we only consider the most stable form of alane,  $\alpha$ - $\text{AlH}_3$ , which decomposes in a single endothermic reaction [4]:



Graetz and Reilly [4,5] and Graetz et al. [6] demonstrated that during the decomposition of the  $\beta$  and  $\gamma$  polymorphs they transition to the  $\alpha$  phase at about  $100^\circ\text{C}$ . After further heating, the  $\alpha$  phase decomposes to  $\text{H}_2$  gas and aluminum. For the temperature range conducted in their study ( $60 < T < 160^\circ\text{C}$ ), Graetz and Reilly [4] determined that the kinetics of the aluminum hydride polymorphs were controlled by nucleation and growth in two and three dimensions and not by the diffusion of  $\text{H}_2$  through a surface oxide. Similarly, Ismail and

Hawkins [7] determined that the single endothermic reaction of alane decomposition proceeds in two steps: 1) a rate limiting two-dimensional nucleation reaction and 2) growth of crystals. Ismail and Hawkins also determined that after the hydrogen is liberated from the particle the resulting products are amorphous and crystalline aluminum. Numerous studies [4–8] at heating rates on the order of a few Kelvin per minute to tens of Kelvin per minute found that the onset of decomposition occurred between 400 and 500 K. In two separate studies, Bazyn et al. [8,9] proposed that in general combustion environments aluminum hydride would react via a two-step mechanism, with the first step being the decomposition reaction shown in Eq. (1) and the second step given by Eq. (2):



In shock-tube studies, Bazyn et al. [9] concluded that the decomposition step occurs significantly faster than ignition and that once the hydrogen has been released the remaining aluminum burns similarly to traditional aluminum of similar size (micron scale).

Il'in et al. [10] studied the products of combustion of alane in air and found that  $\text{AlH}_3$  combustion in air had three stages: 1) a hydrogen flame, separated from the sample with a nonluminous zone; 2) a stage in which, once the hydrogen was consumed, the flame descended and touched the sample resulting in ignition and low-temperature combustion, similar to ultradispersed aluminum powder (UDAP); and 3) a high-temperature stage in which the sample reached  $2000$ – $2400^\circ\text{C}$ . Il'in et al. analyzed the final combustion products and found a substantial amount of  $\text{AlN}$  content, which was consistent with earlier studies on UDAP.

More recently, we studied the decomposition and ignition behavior of alane at much higher heating rates ( $10^4$ – $10^5$  K/s) than previously published [11] by filament heating. During our study, we found that the ignition temperature of alane was a function of heating rate, but it was very similar to that of nanoaluminum while having a particle size ranging from a few microns to more than 20 microns. In addition, at these higher heating rates we found that the decomposition of alane became limited by the transport of hydrogen gas through the aluminum crystal.

Loose-powder nanocomposite thermites are currently being investigated for uses in propellants, pyrotechnics, and explosives. Nanoaluminum-based thermites give rise to high adiabatic flame

Received 11 March 2013; accepted for publication 2 April 2013; published online 31 December 2013. This material is declared a work of the U.S. Government and is not subject to copyright protection in the United States. Copies of this paper may be made for personal or internal use, on condition that the copier pay the \$10.00 per-copy fee to the Copyright Clearance Center, Inc., 222 Rosewood Drive, Danvers, MA 01923; include the code 1533-3876/13 and \$10.00 in correspondence with the CCC.

\*RDT&E Directorate; gregory.young1@navy.mil.

<sup>†</sup>Research Assistant, Department of Mechanical Engineering; sullivan34@lml.gov.

<sup>‡</sup>Research Assistant, Department of Mechanical Engineering; nwp2@umd.edu.

<sup>§</sup>Professor, Department of Chemical Engineering; mrz@umd.edu.

temperatures and produce relatively low amounts of gas. Whereas the reaction mechanism in nanocomposite thermites remains poorly understood, the mode of energy propagation is speculated to be via convection of hot gases [12–14]. One potential way to enhance the reactivity of thermites is to introduce a gas generating constituent, provided that it does not affect the kinetic timescales of the system. We have shown that nanoboron can enhance the reactivity of nanoaluminum–CuO thermites in a recent publication [15], but only when boron was added as the minor component of the fuel. The goal of the current work is to investigate whether aluminum hydride can also enhance the reactivity of a nanoaluminum–CuO system. As discussed, an attractive characteristic of aluminum hydride is its ability to release hydrogen upon thermal decomposition at a relatively low temperature. The liberated hydrogen may therefore serve to enhance the reactivity by improving both the pressurization and convective mode of energy propagation.

## II. Experimental Approach

For this work, thermite samples were prepared with the fuel being composites of nanoaluminum,  $\alpha$ -aluminum hydride with nanoaluminum, micron-sized aluminum with nanoaluminum, and the oxidizers, which consist of copper oxide (CuO), iron oxide (Fe<sub>2</sub>O<sub>3</sub>), and bismuth trioxide (Bi<sub>2</sub>O<sub>3</sub>). In each case, nanoaluminum was the predominant fuel with aluminum hydride or micron-sized aluminum added as a minor component. The minor components were added in terms of the molar percentage of either in the fuel. For example, a 30% AlH<sub>3</sub> sample meant that 30% of the fuel was aluminum hydride, 70% was nanoaluminum, and the corresponding amount of oxidizer was added to make the mixture of interest. In the case of experiments using AlH<sub>3</sub>, the calculated stoichiometry assumed that any hydrogen produced did not participate in the reaction such that the final products of combustion were Al<sub>2</sub>O<sub>3</sub>, H<sub>2</sub>, and the respective metal corresponding to the oxidizer of interest. The nanoaluminum used was obtained from the Argonide Corporation and designated as “50 nm ALEX” by the supplier. ALEX is a nanosized aluminum formed from the electroexplosion of an aluminum wire [16]. Thermogravimetric analysis (TGA) was performed on the ALEX samples to determine the amount of elemental metal (active content) in the particles. TGA showed the ALEX to be 70% active. As previously mentioned, the alane used in this study was  $\alpha$ -alane, rhombohedral crystals that ranged from a few microns to approximately 25  $\mu$ m in size, as seen in Fig. 1. The methods for synthesis and stabilization of the as-received  $\alpha$ -alane used in the study are not fully known to us, although it is likely to have been the same as the material studied by Ismail and Hawkins [7] and Bazyn et al. [8,9]. Because the alane used in this study was on the micron scale, we also substituted micron-sized aluminum in place of the nanoaluminum to make a direct comparison. The micron-sized aluminum was obtained from Atlantic Equipment Engineers and had a size of 1–5  $\mu$ m as per the supplier. The oxidizers copper(II) oxide, iron(III) oxide, and bismuth(III) oxide nanopowders were all purchased from Sigma Aldrich and had an average primary particle

diameter specified by the supplier to be <50, <50, and 90–210 nm, respectively.

The nanocomposite thermites were prepared by mixing the fuel and oxidizer in hexane and sonicating for 20 min to ensure mixing. The hexane was then allowed to dry, and the sample was gently broken apart with a spatula until the consistency for each sample was that of a loose powder.

Three different experimental techniques were used to evaluate the reactivity of alane-based thermite formulations. First, we used the pressurization rate inside a small combustion cell as a measurement of the reactivity. A fixed mass (25 mg) of the sample powder was placed inside a constant-volume (~13 mL) pressure cell. A schematic and more details of the pressure cell can be found in a previous publication [17]. A nichrome wire coupled to a voltage supply was placed in contact with the top of the powder and served as an ignition source through resistive heating of the wire. A piezoelectric pressure transducer was used in series with an inline charge amplifier and a signal conditioner, and the resultant voltage trace was captured on an oscilloscope upon ignition of the sample. The pressurization rate was calculated by converting the voltage rise to pressure and dividing by the rise time in microseconds. This was repeated three times for each sample, and the average pressurization rate (in psi/ $\mu$ s) was recorded. Reference [15] provides a detailed interpretation of the typical pressure signal.

To extract the rise time in a consistent way, we always took the first major peak in the system (usually the maximum voltage) and applied a linear fit. We have reported the average of three tests, and the uncertainty was calculated from the standard deviation of the data.

The decomposition behavior of the AlH<sub>3</sub>-based thermite under rapid heating was investigated by coupling a temperature jump ( $T$  jump) [18] with a time-of-flight (TOF) mass spectrometer [19]. The  $T$  jump employs a ~76  $\mu$ m-diam platinum wire, which is resistively heated at a rate of up to  $\sim 6 \times 10^5$  K/s. This experimental setup has been described thoroughly in [19]. We used this technique to characterize the release of H<sub>2</sub> in alane as well as the decomposition of the corresponding oxidizer when mixed together in the form of a nanocomposite thermite.

Finally, we measured flame propagation velocity in a burn tube to compare the performance of the AlH<sub>3</sub>-based thermite with the standard nanoaluminum thermite. Previously, such tests have been conducted by Bockmon et al. [14] for various nanoaluminum–oxidizer mixtures to study the burn rates for various thermites. Our experimental setup is similar to the one used by Bockmon et al., except that we used two photodiodes at known distances from each other to calculate the average velocity. The light emission was recorded on an oscilloscope as the flame front passed the photodiodes. From the photodiode signal, we selected 5% of the maximum signal as the measure of time for when the flame front passed. The flame propagation velocity was then calculated by dividing the distance between photodiodes by the time difference between the two photodiodes to achieve 5% of maximum signal intensity. The packing densities for the mixtures were approximately 10% of the theoretical maximum density for the thermite mixtures.

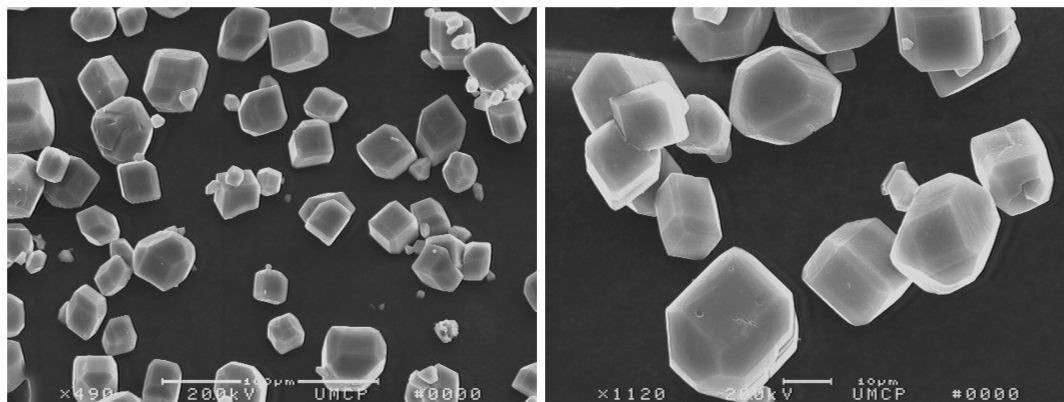


Fig. 1 Scanning electron microscopy image of  $\alpha$ -aluminum hydride.

### III. Results

#### A. Combustion Studies

In this study, we considered baseline thermites of nanoaluminum–metal oxides and incrementally replaced the nanoaluminum with micron-scale  $\alpha$ -aluminum hydride and in some cases micron-scale aluminum. Initially, we used stoichiometric mixtures of the thermites and tested them in our pressure cell to determine the relative performance as a function of alane content. In some cases, the result was an increase in performance, which defined an optimum amount of additive. Initially, it was uncertain whether the  $H_2$  released from the system would oxidize to form  $H_2O$  during the initial pressure rise of our constant-volume experiment. To gain some insight into the role of  $H_2$  in the system, we tested two samples using  $CuO$  as the oxidizer. In one sample, we assumed a stoichiometry in which the products included  $H_2$ , and in the other we provided sufficient oxidizer for the products to form  $H_2O$ . The mixture, which assumed  $H_2$  in the product, was found to be more reactive (i.e., gave higher pressurization rates) than the mixture that assumed  $H_2O$ . Therefore, we only considered the aluminum content in the alane as reactive. Figure 2 shows the results of stoichiometric mixtures of alane as an additive to nanoaluminum–metal-oxide thermites in terms of pressurization rates in a constant-volume pressure cell. In addition, Fig. 2 shows the relative performance when micron-sized aluminum replaces nanoaluminum in a  $CuO$  based thermite. The pressurization rates have been normalized by the pressurization rate of a pure nanoaluminum–corresponding metal oxide thermite.

As Fig. 2 shows, the addition of micron-scale aluminum hydride to a nanoaluminum–copper-oxide thermite enhances the pressurization rate of the nanocomposite thermite, whereas adding aluminum in a similar size decreases the pressurization rate. The decrease in pressurization rate from the baseline thermite of the micron aluminum substituted thermite can be attributed to the time scales associated with micron-sized aluminum combustion. Because micron-sized aluminum takes significantly longer to burn than the nanoaluminum, the addition of micron-sized aluminum slows down the heat release rate relative to the nanoaluminum, thus reducing the performance.

At its optimum performance (20–30%  $AlH_3$ ), the alane– $CuO$  nanocomposite thermite had a pressurization rate that is about a factor of two greater than the baseline nanoaluminum thermite even though it is on the same size scale as the micron-sized aluminum. After about 30%  $AlH_3$  by mole, the pressurization rate decreases dramatically to well below the levels observed with 100% nanoaluminum. The increase in pressurization rate over the baseline with alane can at least partially be attributed to the increased gas production associated with alane decomposition, which proceeds as shown in Eq. (2). In

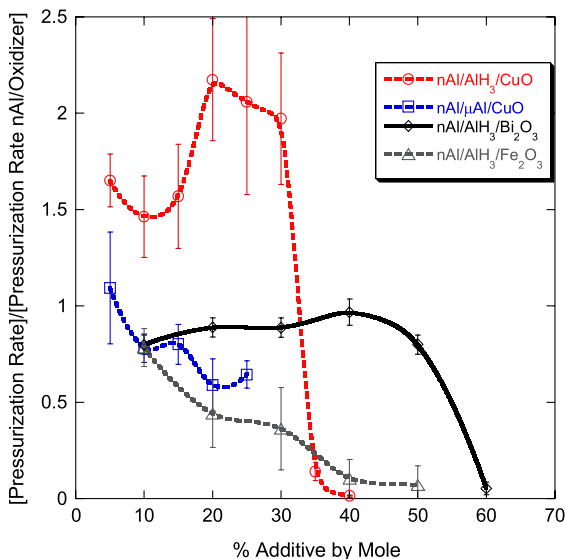


Fig. 2 Normalized pressurization rate as a function of fuel additive for stoichiometric mixtures.

shock-tube studies, Bazyn et al. [9] concluded that the dehydrogenation of alane occurs significantly faster than the ignition process, which would imply a significant amount of gas is produced just before ignition. However, thermochemically, the effect of increasing alane content is to lower the adiabatic flame temperature due to the endothermic decomposition of alane. Whereas thermochemically the alane serves to continue to produce gas, the extended time scales of the remaining micron-scale aluminum and the decrease in flame temperature at some point become the controlling parameters on performance. The thermochemical behavior of two types of  $CuO$ – $nAl$ – $AlH_3$  nanocomposite thermite systems is shown in terms of adiabatic flame temperature in Fig. 3. The first provides enough  $CuO$  to oxidize all of the fuel including the hydrogen gas generated from alane decomposition. The second contains only enough  $CuO$  to oxidize all of the aluminum in the system. Figure 3 demonstrates two interesting features. As mentioned earlier, the addition of alane decreases the flame temperature in both systems. Furthermore, the adiabatic flame temperature of the system containing enough  $CuO$  to oxidize the hydrogen gas to water vapor becomes considerably lower than having hydrogen gas as one of the main combustion products under equilibrium conditions. This does not necessarily mean that the hydrogen does not participate in the thermite reaction. It is quite possible that the hydrogen may react with oxygen and/or the metal oxide as an intermediate step, but in either case the flame temperature is highest when hydrogen is one of the primary combustion products as opposed to water vapor. This in part may help to explain some of our results of an optimum system that contains only enough oxidizer to react with the aluminum. As the flame temperature drops with the addition of  $CuO$  to balance the entire system (i.e., react the hydrogen), the flame temperature begins to approach the vaporization temperature of aluminum. In the event that the flame temperature drops below the vaporization temperature of aluminum, a change in combustion mechanism would take place. The system would have transitioned from homogeneous to heterogeneous reactions, which would significantly slow down the reaction rate, resulting in poor performance, as observed in the experiments.

Interestingly, the alane thermite using  $Fe_2O_3$  and  $Bi_2O_3$  did not show the same enhancement in pressurization rate that the copper oxide thermite did. In fact, the nanocomposite thermite based on  $Fe_2O_3$  saw a dramatic decrease in pressurization rate almost immediately as alane is added. A simple thermochemical analysis, shown in Fig. 4, provides a possible explanation for the poor performance of the  $Fe_2O_3$  system. Again, the addition of alane reduces the flame temperature to levels near or even below the vaporization temperature of aluminum, resulting in a shift of the combustion mechanism from homogeneous to heterogeneous. At the same time, the  $Bi_2O_3$  based nanocomposite thermite appeared relatively insensitive to the addition of alane in terms of

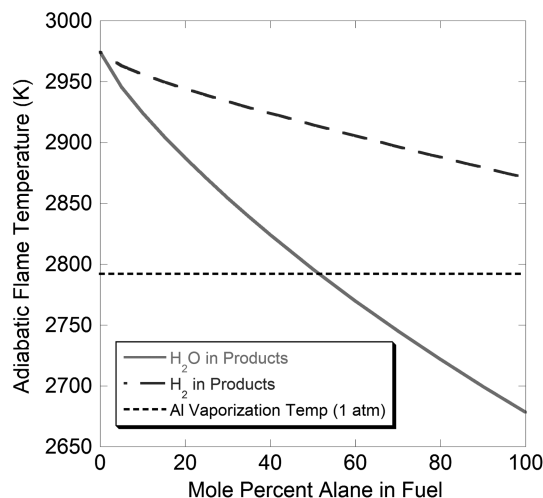


Fig. 3 Calculated adiabatic flame temperatures of  $CuO$ – $nAl$ – $AlH_3$  mixtures.

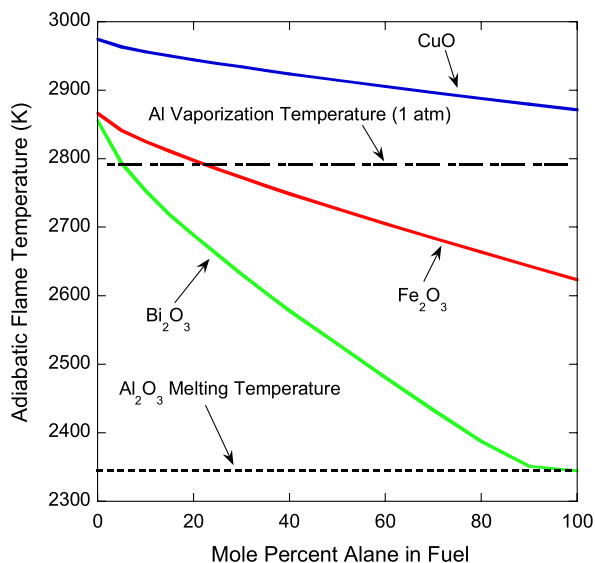


Fig. 4 Calculated adiabatic flame temperatures of alane thermite systems with different metal oxides.

pressurization rate all the way up to about 50%  $\text{AlH}_3$  by mole. The calculations in Fig. 4 show that alane has a greater effect in reducing the flame temperature for the  $\text{Bi}_2\text{O}_3$  system. To begin with, the adiabatic flame temperature of the  $\text{Bi}_2\text{O}_3$  system is closer to the vaporization temperature of aluminum. Any addition of alane drops the adiabatic flame temperature immediately below the vaporization temperature of the aluminum. It is quite possible that the  $\text{Bi}_2\text{O}_3$  system is always operating at or below the aluminum vaporization temperature (including the baseline condition with no alane); thus, there is no real shift in the mechanism, and it is always reacting heterogeneously until the flame temperature gets very near the melting temperature of alumina and the pressurization rate remains relatively constant over a broad range.

On the other hand, with the adiabatic flame temperature of the baseline (no alane)  $\text{Fe}_2\text{O}_3$  system slightly higher than the  $\text{Bi}_2\text{O}_3$  system, the baseline case could be operating above the vaporization temperature of aluminum. But, with the addition of alane the flame temperature is immediately driven below the vaporization temperature of aluminum, and relative performance suffers due to a change in the mechanism.

After about 50%  $\text{AlH}_3$ , the pressurization rate of the  $\text{Bi}_2\text{O}_3$  based nanocomposite thermite falls off dramatically, similar to the  $\text{CuO}$  based nanocomposite thermite. Figure 4 indicates that the further increase in alane content drives the adiabatic flame temperature toward the melting point of alumina. Failure to reach this temperature would significantly alter the combustion mechanism, further slowing the reaction rate down. The thermochemical calculations for the  $\text{CuO}$  and  $\text{Fe}_2\text{O}_3$  thermites were performed using the NASA CEA computer codes with the UV option. The calculations for the  $\text{Bi}_2\text{O}_3$  thermites were performed with the CHEETAH code using the constant-volume explosion option.

With the exception of the  $\text{Fe}_2\text{O}_3$  based thermite, all of the other samples had similar pressure signal rise times as the baseline nanoaluminum thermite, as seen in Fig. 5, up until the optimum amount of alane is added. This result implies that the increase in peak pressure observed in the alane thermite occurs on the same time scale as the baseline, meaning that if the increase in peak pressure is solely a result of hydrogen release then the hydrogen release must occur within this time scale. In the case of the  $\text{Fe}_2\text{O}_3$  system, the rise times are immediately higher than the baseline.

## B. Time Resolved Speciation Measurements

During the next part of the study, we employed a  $T$  jump TOF mass spectrometer to gain a better understanding of the decomposition of the alane nanocomposite thermite. During the experiments, the input voltage and resulting current were recorded. From the recorded

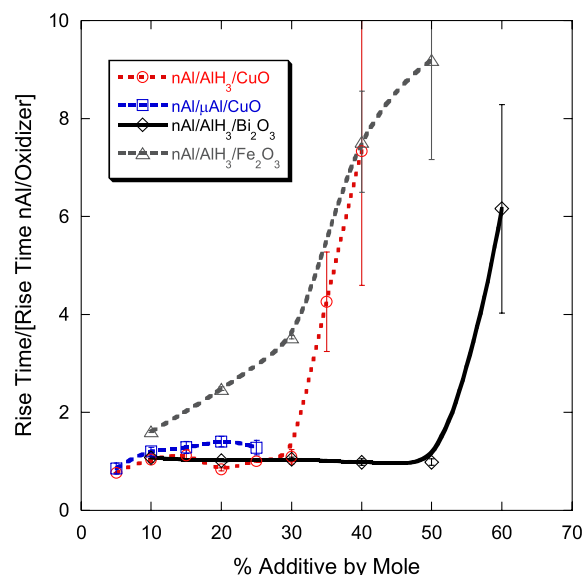


Fig. 5 Rise times of nanocomposite thermites as a function of fuel additive.

voltage and current, and the known length of the platinum wire, the temperature time history can be found as a function of wire resistance using the Callendar–Van-Dusen equation:

$$\frac{R}{R_o} = 1 + \alpha T + \beta T^2 \quad (3)$$

where  $\alpha = 3.91 \times 10^{-3}$ ,  $\beta = -5.78 \times 10^{-7}$ , and  $R_o$  is the reference resistance obtained from the length of the wire at ambient temperature.

Figure 6 shows the temporally resolved mass spectra for the alane-based thermite at a heating rate of  $\sim 6 \times 10^5$  K/s. The spectrum observed at  $t = 0$  ms corresponds to the background and consists primarily of  $\text{H}_2\text{O}$  ( $m/z = 18$ ),  $\text{OH}$  ( $m/z = 17$ ), and  $\text{N}_2$  ( $m/z = 28$ ). Hydrogen and oxygen are clearly observed in the spectra, along with smaller quantities of aluminum. Figures 7 and 8 provide examples of the hydrogen and oxygen temporal release and the evolution of aluminum vapor for a 100% alane fuel thermite and a 25% alane fuel

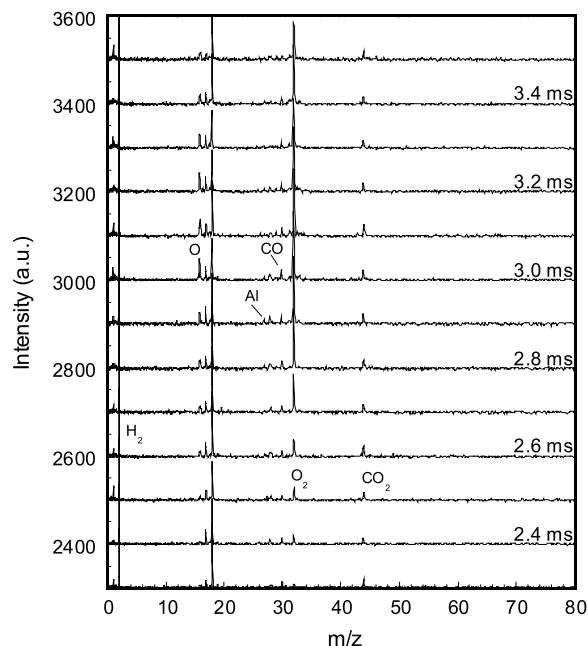


Fig. 6 Temporally resolved  $T$ -jump TOF mass spectra for a heating rate of  $5.7 \times 10^5$  K/s.

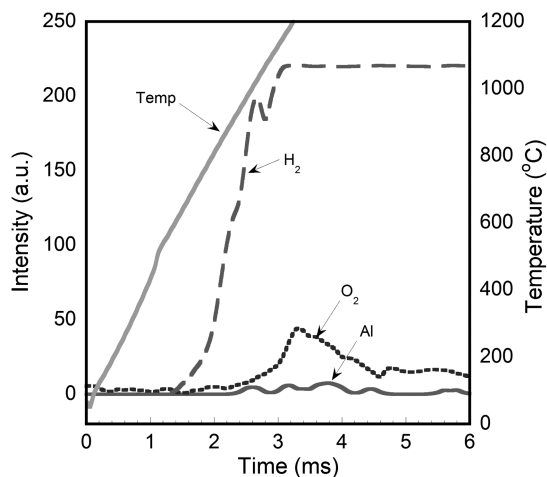


Fig. 7 Species profiles obtained in the  $T$ -jump TOF mass spectrometer for 100%  $\text{AlH}_3$  fuel-CuO thermite.

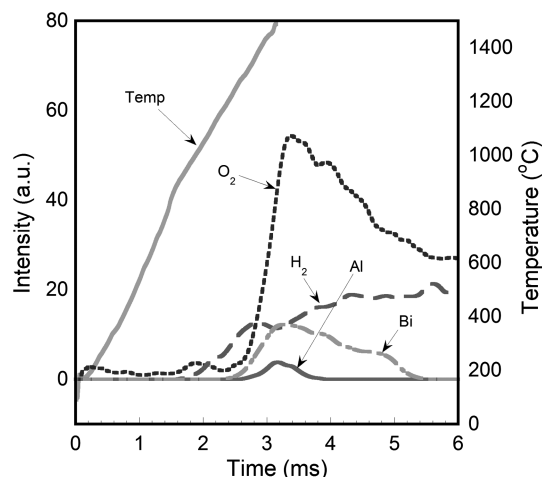


Fig. 9 Species profiles obtained in the  $T$ -jump TOF mass spectrometer for 100%  $\text{AlH}_3$  fuel- $\text{Bi}_2\text{O}_3$  thermite.

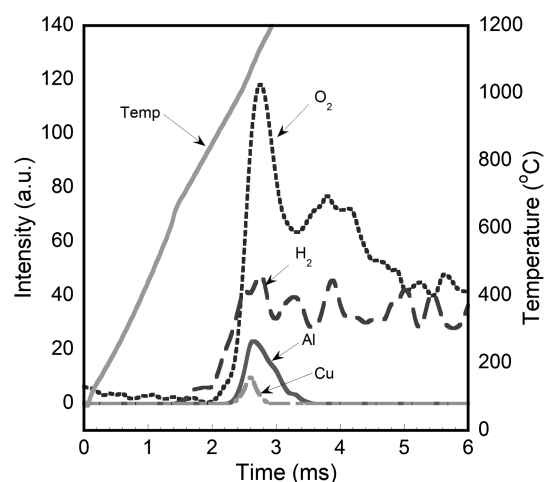


Fig. 8 Species profiles obtained in the  $T$ -jump TOF mass spectrometer for 25%  $\text{AlH}_3$  fuel (balance is nanoaluminum)-CuO thermite.

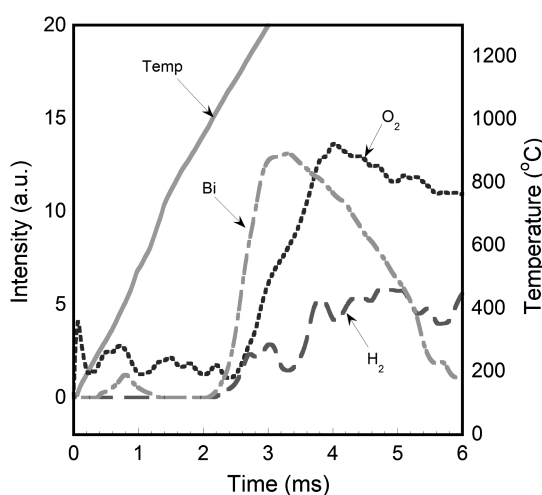


Fig. 10 Species profiles obtained in the  $T$ -jump TOF mass spectrometer for 25%  $\text{AlH}_3$  fuel (balance is nanoaluminum)- $\text{Bi}_2\text{O}_3$  thermite.

(the balance of the fuel was nanoaluminum) nanocomposite thermite, respectively. Interestingly, in both systems the release of  $\text{H}_2$  occurs at approximately the same temperature (see Figs. 7 and 8) and at similar rates. On the other hand, whereas the  $\text{O}_2$  appears to be released at similar temperatures in each sample, the 25% alane fuel mixture clearly shows  $\text{O}_2$  released at much higher rates in comparison with the 100% alane fuel. This is a clear indication of a reaction that is propagating faster (25% alane). The corresponding temperature of the release of hydrogen ranges between  $630^\circ\text{C}$  (903 K) and  $730^\circ\text{C}$  (1003 K) from experiment to experiment with a heating rate of approximately  $6 \times 10^5$  K/s. This is within reasonable agreement with a previous study by Young et al. [11] on the decomposition of alane on its own at similar heating rates. At much lower heating rates, alane decomposition has been shown to begin at much lower temperatures, typically around  $150^\circ\text{C}$  (423 K) [4–8]. The difference in temperature of decomposition can be directly attributed to the heating rates used in this study and consequently the operating temperatures. At the lower heating rates, and thus lower temperatures, chemical kinetics is the rate limiting process; however, as the heating rate is increased, and thus the operating temperature is increased significantly, diffusion or mass transfer becomes the limiting process [11]. Another interesting observation is the presence of copper in the 25% alane mixture, which does not appear in the 100% alane thermite, which is an indicator that the 100% case has a lower flame temperature.

The  $T$ -jump mass spectrometer shows that hydrogen is released from the alane at approximately the same time and temperature as the oxygen from the copper oxide but provides no information to indicate

if hydrogen participates in the reaction with the oxygen or the rest of the thermite mixture. Regardless, however, of whether or not the hydrogen reacts with the oxygen or the metal oxide, our experimental results and thermochemical analysis indicate that the system is optimized when the  $\text{H}_2$  is considered as the product species.

Figures 9 and 10 show the time resolved species profiles for the  $\text{Bi}_2\text{O}_3$  based thermite for the 100 and 25% alane fuels, respectively. In this system, we note that the rate of Bi release is significantly increased for the 25% alane fuel in comparison with the 100% alane case. Again, this demonstrates that the alane is significantly altering the reaction rate of the system, most likely due to a shift in the combustion mechanism between the 25 and 100% alane fuel cases and a higher temperature to form vapor phase Bi. This is supported in the thermochemical calculations shown in Fig. 4. At 25% alane, the flame temperature is between the vaporization temperature of aluminum and the melting temperature of alumina, while at 100% alane the flame temperature has dropped below the melting point of alumina.

Figures 11 and 12 show the time resolved species profiles for the  $\text{Fe}_2\text{O}_3$  based thermite for the 100 and 25% alane fuels, respectively. Unlike the CuO and  $\text{Bi}_2\text{O}_3$  nanocomposite thermites, we do not observe any significant changes in the speciation rates at the two different conditions with  $\text{Fe}_2\text{O}_3$ . Equilibrium calculations suggest that at both of these  $\text{AlH}_3$  loading levels the flame temperature is below the vaporization temperature of aluminum but still above the melting temperature of alumina. Thus, whereas the performance

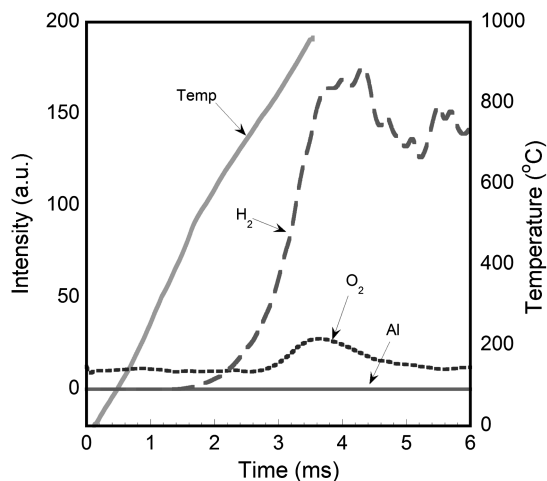


**Fig. 11** Species profiles obtained in the  $T$ -jump TOF mass spectrometer for 100%  $\text{AlH}_3$  fuel- $\text{Fe}_2\text{O}_3$  thermite.

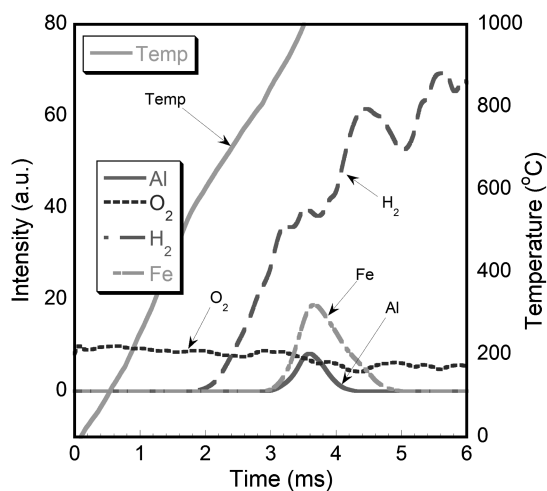


**Fig. 12** Species profiles obtained in the  $T$ -jump TOF mass spectrometer for 25%  $\text{AlH}_3$  fuel (balance is nanoaluminum)- $\text{Fe}_2\text{O}_3$  thermite.

continues to degrade with increasing alane content, the rate of degradation is not as stark as it is in the  $\text{Bi}_2\text{O}_3$  cases studied. This result is consistent with our earlier conclusion that the addition of alane has altered the reaction rate of the  $\text{Fe}_2\text{O}_3$  based thermite and that it is most likely operating as a heterogeneous system with any addition of alane yet still above the melting temperature of alumina.

With comparison with the  $\text{CuO}$  and  $\text{Fe}_2\text{O}_3$  samples, the  $\text{Bi}_2\text{O}_3$ - $\text{AlH}_3$  thermite shows a significant decrease in  $\text{H}_2$  production for both formulations as well as a significant shift to a higher temperature in which  $\text{H}_2$  is detected. This is likely due to the reactive sintering of  $\text{Bi}_2\text{O}_3$  with the alane at a low temperature, before the primary  $\text{H}_2$  release from alane. A reactive sintering mechanism has previously been proposed [20] to explain the initial reaction events of a nanothermite system and is backed by experimental evidence. In this mechanism, the metal oxide particles go through a low-temperature sintering process to create an intimate contact between the aluminum and metal oxide particles, which promotes initiation of the main nanothermite reaction. The  $\text{Al}$ - $\text{Bi}_2\text{O}_3$  system has the lowest decomposition temperature compared with the  $\text{CuO}$  and  $\text{Fe}_2\text{O}_3$  containing nanothermites and reacts at a temperature below the melting point of bulk aluminum (933 K) and  $\text{Bi}_2\text{O}_3$  (1097 K). Whereas this study does not confirm the temperature of sintering, it is believed to be well below that of the ignition point of  $\text{Al}$ - $\text{Bi}_2\text{O}_3$  at  $\sim 857$  K. Sintering of nanoparticles is typically thought to be possible at the Tammann temperature, or  $0.5T_{\text{melt}}$  (where  $T_{\text{melt}}$  is the melting

point of a bulk sample), which for  $\text{Bi}_2\text{O}_3$  is  $\sim 549$  K [21]. Another study on  $\text{Al}$ - $\text{Bi}_2\text{O}_3$  nanothermites showed that during heating of a mixture of  $\text{Bi}_2\text{O}_3$  and  $\text{CuO}$  nanoparticles the gaseous  $\text{O}_2$  release from  $\text{CuO}$  was significantly reduced. It was concluded that  $\text{Bi}_2\text{O}_3$ , which has a lower melting point than that of copper oxide, sinters over the  $\text{CuO}$  to prohibit the release of gaseous  $\text{O}_2$  [22]. With a Tammann temperature below the temperature of  $\text{H}_2$  release, it is reasonable to conclude that this process is occurring in the  $\text{Bi}_2\text{O}_3$  containing nanocomposite thermite, prohibiting the release of  $\text{H}_2$  gas.

### C. Flame Velocity

We also examined the effect of alane on the propagation velocity of the nanocomposite thermite in a burn tube test [14]. Taking our optimum mixture (25% alane by mole) with an equivalence ratio of one (again assuming the hydrogen does not take part in the reaction), we found that the propagation velocity was increased with alane (680 m/s) by about 21% over that of the baseline nanoaluminum-copper-oxide thermite (560 m/s).

Whereas the mass spectrometer results indicate a simultaneous release of  $\text{O}_2$  and  $\text{H}_2$ , with a time resolution of  $\sim 100 \mu\text{s}$ , bulk materials (from pressure cell data) show rise times an order of magnitude faster and are nominally associated with convective heat transfer effects. Thus, for bulk flame propagation small differences in the  $\text{H}_2$  vs  $\text{O}_2$  release may in fact be significant. If  $\text{H}_2$  is released first it should, based on higher thermal conductivity and diffusivity, be a very effective medium for convective heat transfer.

Therefore, the benefit of alane to a nanocomposite thermite may be twofold: first, the increased gas production from decomposition of alane, and second, the increase in heat transfer rates associated with  $\text{H}_2$  convection. Thus, the increased burning rate occurs despite the fact that the adiabatic flame temperature is lower.

## IV. Discussion

In this study, we have observed that micron-sized alane can enhance the performance of baseline thermites in terms of pressurization rate and peak pressure in a constant-volume pressure cell and the propagation velocity in a burn tube when it is a minor component of the fuel. At the same time, with similar size aluminum particles we see no enhancement of the baseline thermite in any of the experiments. We have attributed this to the release of hydrogen from the alane contributing to convection heat transfer as a means of enhancement. However, we should also consider that the ignition temperature of alane is very close to that of nanoaluminum ( $\sim 1000$  K) [11,23], whereas micron sized-aluminum typically does not ignite until it reaches  $\sim 2300$  K [24–28]. This would suggest that the aluminum component of alane might also be contributing to the overall heat release of the system through the oxidation of aluminum beginning earlier in time and at a lower temperature in comparison with traditional micron-scale aluminum. However, in shock-tube studies of alane combustion, Bazyn et al. [9] found that after the release of hydrogen the remaining aluminum burns on a similar time scale to that of similarly sized aluminum. Similar to our earlier study [11], we found that burning times were on the order of milliseconds, compared with the microsecond scales expected of nanoaluminum [23]. Thus, whereas there may be a small benefit from earlier and lower starting temperature aluminum oxidation of alane, the overall contribution from the aluminum portion of the alane in our thermite system is likely to be minimal. Our results also showed that there is an optimum amount of alane that can be added (20–30% by mole) to enhance the thermite system. The fact that there is an optimum amount of alane suggests that there is a balance between the positive contribution of the hydrogen in terms of pressurization and convection and the negative aspects of longer burning times not contributing to the main reaction, thus creating an optimum amount of alane above which performance suffers. This would imply that if the alane particles were on the nanoscale rather than the micron scale it would be a far superior fuel to aluminum in a nanocomposite thermite system.

## V. Conclusions

During this study, the effects of the addition of micron-scale alane on the combustion performance of three typical thermite systems, CuO–nAl, Bi<sub>2</sub>O<sub>3</sub>–nAl, and Fe<sub>2</sub>O<sub>3</sub>–nAl, were examined. In constant-volume pressure cell testing, it was found that the addition of alane to a CuO–nAl thermite as a minor fuel component could enhance pressurization rates by a factor of about two. Above approximately 30% alane by mole of fuel, the performance drops off drastically to well below baseline performance. At the same time, the addition of micron-scale aluminum to the CuO–nAl thermite results in a gradual degradation of performance. The enhanced performance of the alanzed thermite can be directly attributed to the release of H<sub>2</sub> upon alane decomposition. The additional gas aids in pressurization and helps to improve the convective heat transfer of the system even though it lowers the adiabatic flame temperature.

The addition of alane to a Bi<sub>2</sub>O<sub>3</sub> based thermite leaves performance largely unaffected until alane becomes the majority fuel component. For an Fe<sub>2</sub>O<sub>3</sub> thermite, alane addition results only in degraded performance at all addition levels. In each case, the performance degradation can be attributed to a transition in the combustion mechanism. As an example, once alane is added to the iron oxide thermite, the flame temperature drops below the vaporization temperature of aluminum, resulting in a change from homogeneous to heterogeneous combustion. Similarly, in the bismuth oxide system, at very high loadings of alane, the flame temperature drops below the melting temperature of alumina, thus severely altering the combustion mechanism of the aluminum fuel.

Burn tube studies of an alanzed CuO based thermite found that the propagation velocity of the alanzed thermite was about 25% higher than that of the baseline. The release of hydrogen in the alane increases the amount of gas in the whole system, which would contribute to enhancing the energy propagation in the system by convection.

Alane ultimately lowers the flame temperature of these traditional nanocomposite thermite systems, at the same time improving performance under appropriate conditions. This suggests that a degree of tunability with certain mixtures is possible. Alane's ability to generate additional gas and ignite at low temperatures allows it to enhance performance over more traditional fuels, but with limits. These limits appear to be associated with temperatures that govern the overall combustion mechanism.

## Acknowledgments

This research effort was sponsored through the Center for Energetic Concepts Development, a collaborative effort between the U.S. Naval Surface Warfare Center Indian Head Division and the University of Maryland. Partial support was also obtained from the Office of Naval Research University Laboratory Initiative program and the office of Army Research. Finally, we would like to thank Snehaunshu Chowdhury for his assistance with the burn tube studies.

## References

- [1] Petrie, M. A., Bottaro, J. C., Schmitt, R. J., Penwell, P. E., and Bomberger, D. C., "Preparation of Aluminum Hydride Polymorphs, Particularly Stabilized  $\alpha$ -AlH<sub>3</sub>," U.S. Patent No. US 6,228,338 B1, 8 May 2001.
- [2] Brower, F. M., Matzek, N. E., Reigler, P. F., Rinn, H. W., Roberts, C. B., Schmidt, D. L., Snover, J. A., and Terada, K., "Preparation and Properties of Aluminum Hydride," *Journal of the American Chemical Society*, Vol. 98, No. 9, 1976, pp. 2450–2453. doi:10.1021/ja00425a011
- [3] Sinke, G. C., Walker, L. C., Oeting, F. L., and Stull, D. R., "Thermodynamic Properties of Aluminum Hydride," *Journal of Chemical Physics*, Vol. 47, No. 8, 1967, pp. 2759–2761. doi:10.1063/1.1712294
- [4] Graetz, J., and Reilly, J. J., "Decomposition Kinetics of the AlH<sub>3</sub> Polymorphs," *Journal of Physical Chemistry B*, Vol. 109, No. 47, 2005, pp. 22181–22185. doi:10.1021/jp0546960
- [5] Graetz, J., and Reilly, J. J., "Thermodynamics of the  $\alpha$ ,  $\beta$ , and  $\gamma$  Polymorphs of AlH<sub>3</sub>," *Journal of Alloys and Compounds*, Vol. 424,

- Nos. 1–2, 2006, pp. 262–265. doi:10.1016/j.jallcom.2005.11.086
- [6] Graetz, J., Reilly, J. J., Kulleck, J. G., and Bowman, R. C., "Kinetics and Thermodynamics of the Aluminum Hydride Polymorphs," *Journal of Alloys and Compounds*, Vols. 446–447, Oct. 2007, pp. 271–275. doi:10.1016/j.jallcom.2006.11.205
- [7] Ismail, I. M. K., and Hawkins, T., "Kinetics of Thermal Decomposition of Aluminum Hydride, 1: Non-Isothermal Decomposition Under Vacuum and in Inert Atmosphere (Argon)," *Thermochimica Acta*, Vol. 439, Nos. 1–2, 2005, pp. 32–43. doi:10.1016/j.tca.2005.08.029
- [8] Bazyn, T., Krier, H., Glumac, N., Shankar, N., Wang, X., and Jackson, T. L., "Decomposition of Aluminum Hydride Under Solid Rocket Motor Conditions," *Journal of Propulsion and Power*, Vol. 23, No. 2, 2007, pp. 457–464. doi:10.2514/1.22920
- [9] Bazyn, T., Eyer, R., Krier, H., and Glumac, N., "Combustion Characteristics of Aluminum Hydride at Elevated Pressure and Temperature," *Journal of Propulsion and Power*, Vol. 20, No. 3, 2004, pp. 427–431. doi:10.2514/1.3160
- [10] Il'in, A. P., Bychin, N. V., and Gromov, A. A., "Products of Combustion of Aluminum Hydride in Air," *Combustion, Explosion, and Shock Waves*, Vol. 37, No. 4, 2001, pp. 490–491. doi:10.1023/A:1017973601611
- [11] Young, G., Piekielek, N., Chowdhury, S., and Zachariah, M. R., "Ignition Behavior of  $\alpha$ -AlH<sub>3</sub>," *Combustion, Science, and Technology*, Vol. 182, No. 9, Sept. 2010, pp. 1341–1359. doi:10.1080/00102201003694834
- [12] Son, S. F., Asay, B. W., Foley, T. J., Yetter, R. A., Wu, M. H., and Risha, G. A., "Combustion of Nanoscale Al/MoO<sub>3</sub> Thermite in Micro-channels," *Journal of Propulsion and Power*, Vol. 23, No. 4, 2007, pp. 715–721. doi:10.2514/1.26090
- [13] Asay, B. W., Son, S. F., Busse, J. R., and Oschwald, D. M., "Observations on the Mechanism of Reaction Propagation in Metastable Intermolecular Composites," *AIP Conference Proceedings*, Vol. 706, 2004, pp. 827–830. doi:10.1063/1.1780364
- [14] Bockmon, B. S., Pantoya, M. L., Son, S. F., Asay, B. W., and Mang, J. T., "Combustion Velocities and Propagation Mechanisms of Metastable Interstitial Composites," *Journal of Applied Physics*, Vol. 98, No. 6, 2005, Paper 064903. doi:10.1063/1.2058175
- [15] Sullivan, K., Young, G., and Zachariah, M. R., "Enhanced Reactivity of Nano-B/Al/CuO MIC's," *Combustion and Flame*, Vol. 156, No. 2, 2009, pp. 302–309. doi:10.1016/j.combustflame.2008.09.011
- [16] Katz, J., Tepper, F., Ivanov, G. V., Lerner, M. I., and Davidovich, V., "Metastable Nanosize Aluminium Powder as a Reactant in Energetic Formulations," *CPIA Publication 675, JANNAF Propulsion Meeting*, Vol. 3, 1998, pp. 343–349.
- [17] Prakash, A., McCormick, A. V., and Zachariah, M. R., "Synthesis and Reactivity of a Super-Reactive Metastable Intermolecular Composite Formulation," *Advanced Materials*, Vol. 17, No. 7, 2005, pp. 900–903. doi:10.1002/(ISSN)1521-4095
- [18] Brill, T. B., Brush, P. J., James, K. J., Shepherd, J. E., and Pfeiffer, K. J., "T-Jump/FT-IR Spectroscopy: A New Entry into the Rapid, Isothermal Pyrolysis Chemistry of Solids, and Liquids," *Applied Spectroscopy*, Vol. 46, No. 6, 1992, pp. 900–911. doi:10.1366/0003702924124277
- [19] Zhou, L., Piekielek, N., Chowdhury, S., and Zachariah, M. R., "T-Jump/Time-of-Flight Mass Spectrometry for Time-Resolved Analysis of Energetic Materials," *Rapid Communications in Mass Spectrometry*, Vol. 23, No. 194, 2009, pp. 194–202. doi:10.1002/rcm.3815
- [20] Sullivan, K. T., Piekielek, N. W., Wu, C., Chowdhury, S., Kelly, S. T., Hufnagel, T. C., Fezzaa, K., and Zachariah, M. R., "Reactive Sintering: An Important Component in the Combustion of Nanocomposite Thermites," *Combustion and Flame*, Vol. 159, No. 1. doi:10.1016/j.combustflame.2011.07.015
- [21] Satterfield, C. N., "Heterogeneous Catalysis in Industrial Practice," 2nd ed., McGraw-Hill, New York, 1991.
- [22] Piekielek, N. W., Zhou, L., Sullivan, K. T., Chowdhury, S., Egan, G., and Zachariah, M. R., "Initiation and Reaction in Al/Bi<sub>2</sub>O<sub>3</sub> Nanothermites: Evidence for Condensed Phase Chemistry" (submitted for publication).
- [23] Bazyn, T., Krier, H., and Glumac, N., "Combustion of Nanoaluminum at Elevated Pressure and Temperature Behind Reflected Shock Waves,"

- Combustion and Flame*, Vol. 145, No. 4, 2006, pp. 703–713.  
doi:10.1016/j.combustflame.2005.12.017
- [24] Brossard, C., Ulas, A., Yen, C. L., and Kuo, K. K., “Ignition and Combustion of Isolated Aluminum Particles in the Post-Flame Region of a Flat-Flame Burner,” *16th International Colloquium on the Dynamic Explosions and Reactive Systems*, Krakow, Poland, 1997.
- [25] Brzustowski, T. A., and Glassman, I. “Spectroscopic Investigation of Metal Combustion,” *Progress in Astronautics and Aeronautics*, Vol. 15, 1964, pp. 15–75.
- [26] Friedman, R., and Macek, A. “Ignition and Combustion of Aluminum Particles in Hot Ambient Gases,” *Combustion and Flame*, Vol. 6, 1962, pp. 9–19.  
doi:10.1016/0010-2180(62)90062-7
- [27] Friedman, R., and Macek, A., “Combustion Studies of Single Aluminum Particles,” *Proceedings of the Combustion Institute*, Vol. 9, No. 1, 1963, pp. 703–709.
- [28] Kuehl, D. K., “Ignition and Combustion of Aluminum and Beryllium,” *AIAA Journal*, Vol. 3, No. 12, 1965, pp. 2239–2247.  
doi:10.2514/3.3352

S. Son  
Associate Editor